ACS Catalysis

pubs.acs.org/acscatalysis Research Article

Alkene-Chelated Ruthenium Alkylidenes: A Missing Link to New Catalysts

Saswata Gupta,[‡] Venkata R. Sabbasani,[‡] Siyuan Su, Donald J. Wink, and Daesung Lee*

Cite This: *ACS Catal.* 2021, 11, 1977−1987 Read Online

ACCESS | Metrics & More | Article Recommendations | Supporting Information

ABSTRACT: A variety of heteroatom-chelated ruthenium alkylidenes have been developed as metathesis-active catalysts. Alkene-chelated ruthenium alkylidenes, however, have not been considered as a viable alternative because alkene coordination is a necessary step in the catalytic cycle. Relying on common design principles with varying steric and electronic factors, a series of structurally diverse alkene-chelated ruthenium alkylidene complexes were prepared by trapping the intermediates of enyne ring-closing metathesis (RCM) of 1,*n*-enynes and diynes with a stoichiometric amount of an initiator ruthenium complex. One of the crucial structural elements that promotes the formation of 1,5-alkene-chelates is the *exo*-Thorpe−Ingold effect, exerted by a *gem*-dialkyl moiety. These alkene-chelated complexes show a trans relationship between the *N*-heterocyclic carbene (NHC) ligand and the chelated alkene. On the other hand, η^3-vinyl alkylidene complexes were generated from the RCM of ynamide-tethered 1,*n*-enynes. The presence of an ynamide moiety with a right connectivity is essential for the formation of these rare η^3-vinyl alkylidene complexes with a cis relationship between the *N*-heterocyclic carbene (NHC) ligand and the chelated alkene. The stability and reactivity of these alkene-chelated ruthenium alkylidenes could be finely tuned to show characteristic behaviors in RCM, cross-metathesis (CM), and ring-opening metathesis polymerization (ROMP) reactions.

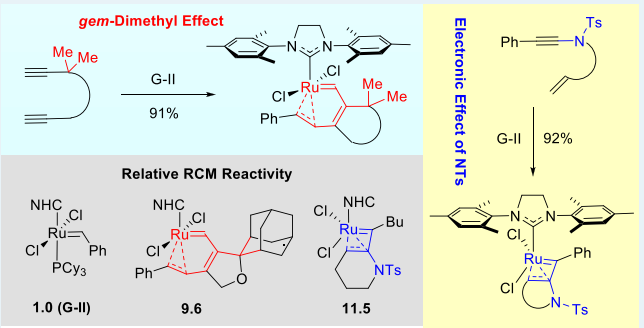

KEYWORDS: *ruthenium alkylidenes, enyne metathesis, exo-Thorpe−Ingold effect, η^3-vinyl alkylidene, ynamides, gem-dialkyl effect*

INTRODUCTION

Olefin metathesis is a powerful and atom-economical synthetic tool[1] for the construction of carbon−carbon double bond and its paramount impacts in many areas of research in academia and industry[2] have been recognized by the 2005 Nobel Prize. Among metal-carbene complexes used for metathesis reactions, ruthenium-alkylidene carbenes, known as the Grubbs catalysts (**G-I** and **G-II**),[3] have shown a wide range of applications, especially in complex natural product synthesis,[4] due to relatively high stability and compatibility with polar functional groups. Even in the presence of Lewis basic polar functional groups, the preferred coordination of an alkene or alkyne to the coordinatively unsaturated ruthenium metal center can be realized for productive metathesis. However, too strong coordination events at any intermediate stage may halt the catalytic cycle. While many stable heteroatom-chelated ruthenium alkylidenes[5−8] are known, including the Hoveyda−Grubbs complex (**HG-II**),[9] the corresponding alkene- and alkyne-chelated ruthenium alkylidene complexes are only sporadically reported in the literature.

The first reported alkene-chelated ruthenium alkylidene **1** was isolated by Snapper and co-workers from a ring-opening metathesis of a cyclobutene using **G-I** as a catalyst (Figure 1). This alkene complex has a trans relationship between the chelated alkene and the PCy_3 ligand and can re-enter the metathesis catalytic cycle.[10] Subsequently, Grubbs and co-workers reported two different types of alkene-chelated complexes **2** and **3**/**3′** derived from the cross-metathesis of **G-II** with diphenylacetylene and *o*-vinylstyrene, respectively. In contrast to the trans alkene-binding mode in **1**, both complexes **2** and **3**/**3′** have a cis relationship between the chelated alkene and the NHC ligand. Although the two cis complexes **3** and **3′** are readily exchangeable, the corresponding trans complex has not been observed.[11,12] Recently, Choi and co-workers the isolated alkene-chelated intermediate **4** from cyclopolymerization of 1,8-nonadiyne with **G-III** and **HG-II**, where the chelated alkene and the NHC ligand have a trans relationship.[13] The closely related alkyne-chelated complex **5** was reported by Lee and co-workers, wherein the alkyne coordination mode is also trans to the NHC.[14]

Received: November 15, 2020
Revised: January 16, 2021
Published: February 1, 2021

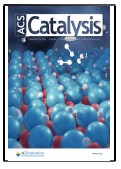

https://dx.doi.org/10.1021/acscatal.0c04972
ACS Catal. 2021, 11, 1977−1987

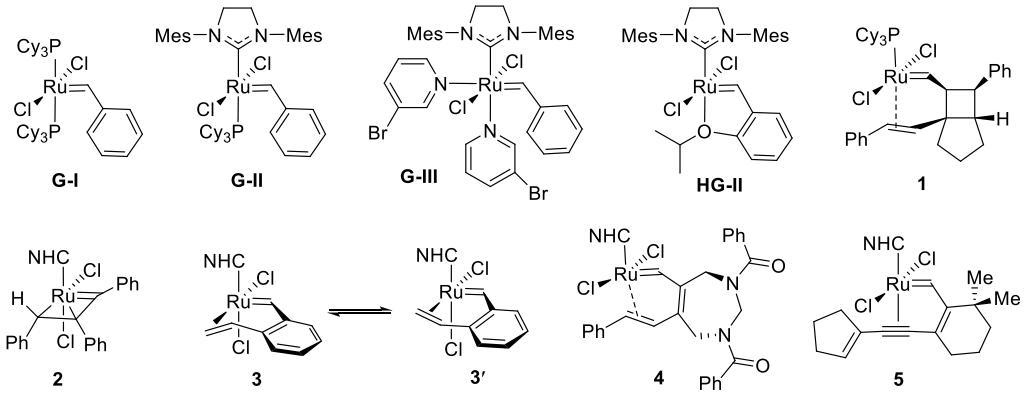

Figure 1. Structures of Grubbs catalysts and previously reported alkene- and alkyne-chelated ruthenium alkylidenes.

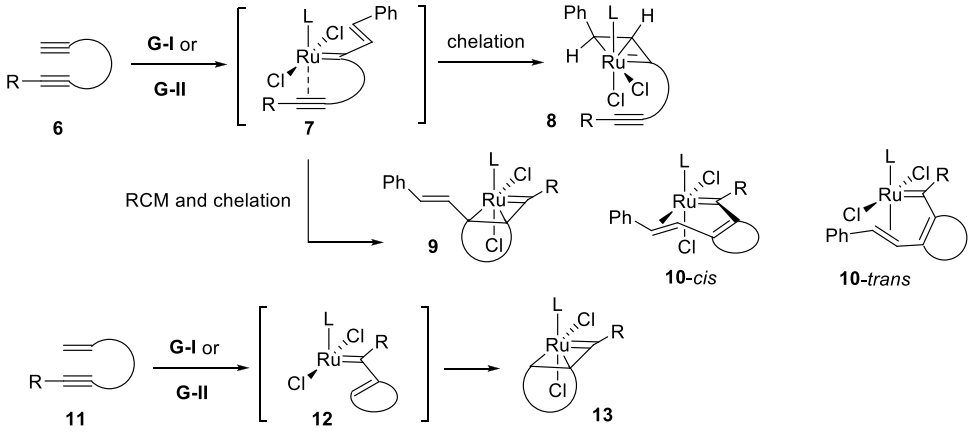

Figure 2. Probable classes of alkene-chelated ruthenium alkylidenes that can be generated through enyne RCM.

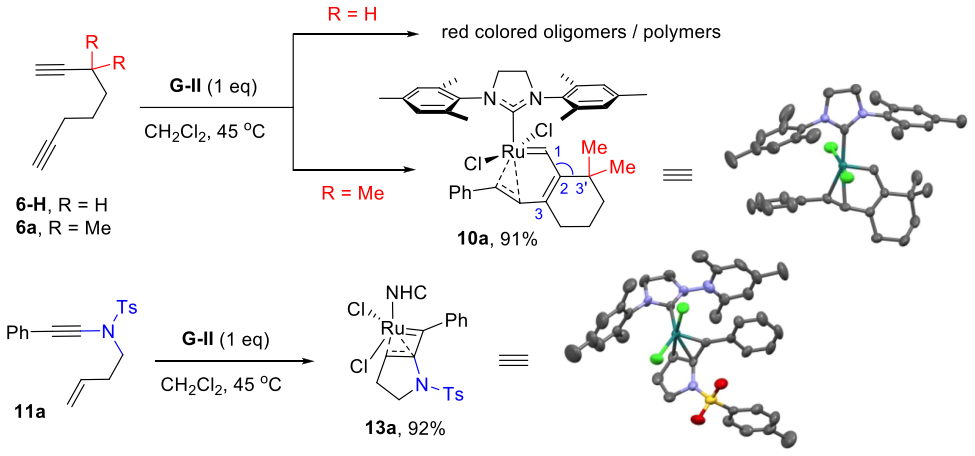

Figure 3. Steric and electronic factors stabilizing alkene-chelates.

Because of the paucity of π-chelated ruthenium alkylidene complexes, it is difficult to generalize the preferred chelation mode of the tethered alkene or alkyne to the ruthenium center, which calls for further investigations. We expect that the preference for different chelation modes should depend on the combined steric and electronic effects of the ligand environment on the metal center.[15] We envisioned that the RCM of 1,*n*-diyne **6** would provide an ideal platform for systematic exploration of the chelation behavior of structurally differentiated ruthenium alkylidenes (Figure 2). It is expected that the CM between the terminal alkyne moieties of **6** and a ruthenium alkylidene initiator, **G-I** or **G-II**, would generate the styryl-substituted alkylidene **7**.[16,17] If the styryl chelation is more preferred than the subsequent ring closure, the complex **7** would be arrested to generate the η^3-vinyl chelate **8**, whereas if the ring closure of **7** is favored, either the η^3-vinyl chelate **9** or 1,5-chelate **10**-*cis/trans* would be generated wherein formation of the latter should be more favorable due to a geometric constraint.[18,19] On the other hand, the RCM of 1,*n*-enyne **11** would generate the alkylidene intermediate **12**, which may be forced to form the η^3-vinyl chelate **13**.[11] The prerequisite for the formation of these alkene-chelates is rapid initiation by a stoichiometric initiator and strong intramolecular interaction of the metal center with the

https://dx.doi.org/10.1021/acscatal.0c04972
ACS Catal. 2021, 11, 1977−1987

Table 1. Tandem CM−RCM of 1,*n*-Diynes to Generate 1,5-Alkene-Chelates

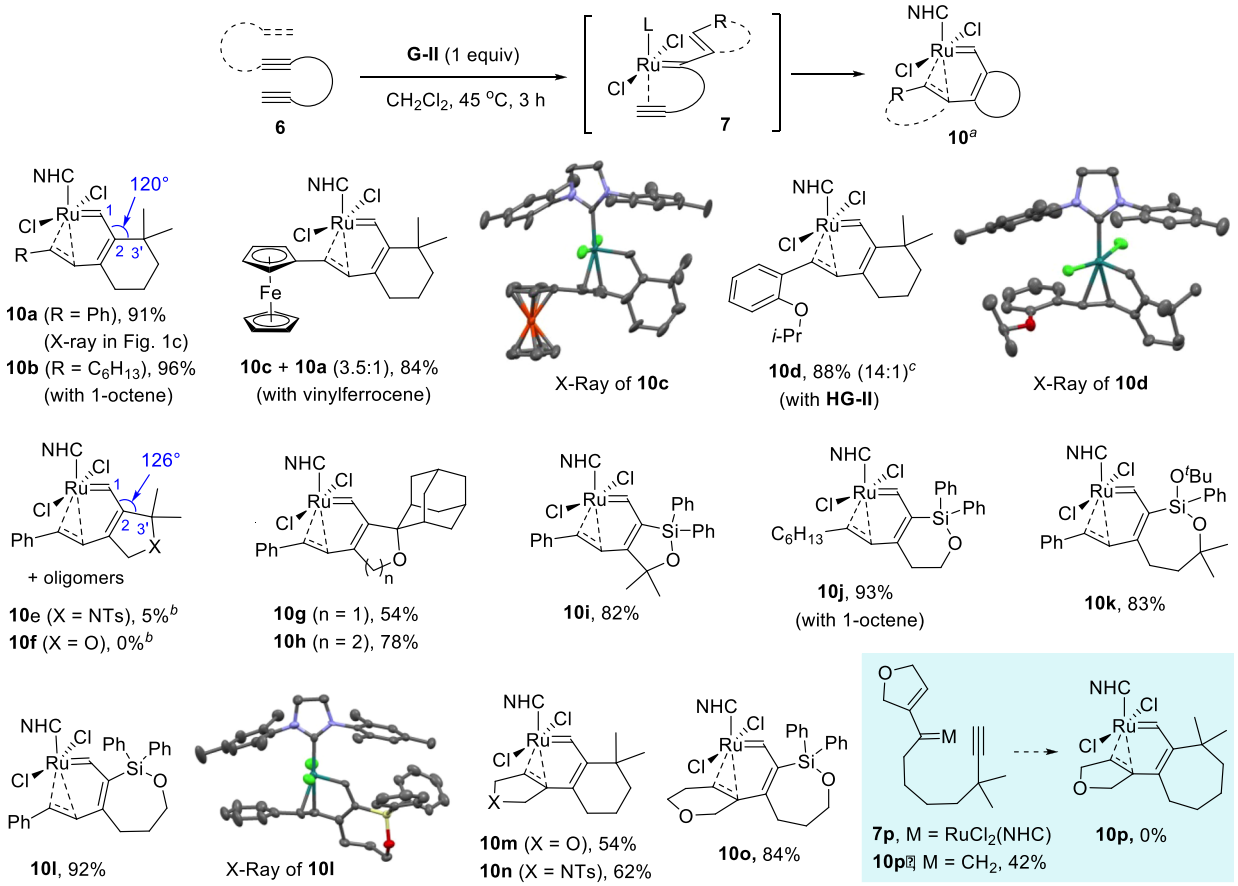

[a]Isolated yield. [b]Mostly oligomers formed. [c]*E*:*Z* ratio.

newly formed double bond such that the next catalytic cycle is halted.

In this study, we focused our exploration on identifying general structural elements that strongly stabilize alkene-chelates. We found that the RCM of diyne **6-H** with **G-II** provided only a polymerized material, while RCM of **6a** led to the formation of **10a**, which is believed to be the consequence of the *exo*-Thorpe−Ingold effect exerted by a *gem*-dialkyl moiety, effectively promoting the alkene chelation (Figure 3).[20,21] This outcome clearly indicates that among the possible chelates **8**−**10**, the six-membered ring chelate **10**-*trans* containing a trans relationship between the *N*-heterocyclic carbene (NHC) ligand and the chelated alkene is the most favorable. This ligand disposition is similar to that of chelate **4**, which does not contain a *gem*-dimethyl group. Also, in the RCM of ynamide-tethered enyne **11a**, the electron-rich nature of an enamide moiety of the intermediate facilitates the formation of η^3-vinyl alkylidene **13a**.[22] These steric and electronic controlling structural elements were exploited for preparation of other related alkene-chelated complexes. The stability and reactivity profiles of these complexes were found to be finely tunable, which is reflected in their catalytic performances in RCM, CM, and ROMP reactions.

RESULTS AND DISCUSSION

Reaction Profile of 1,*n*-Diynes to Generate 1,5-Alkene-Chelates. The contrasting behavior of 1,7-diynes **6-H** and **6a** implies that the *gem*-dimethyl group at the propargylic carbon of **6a** is crucial for forming alkene-chelate **10a** (Figure 3). The structural characteristics of **10a** suggest that the *gem*-dimethyl group should not only restrict the rotation of the C1−C2 bond but also force the metal center to be oriented toward the styryl group at the *β*-position. Although we expected that the *gem*-dimethyl group-based steric effect, the *exo*-Thorpe−Ingold effect, should be a dominating factor to stabilize the alkene chelation in **10a**, the overall stability is likely to depend on other structural factors. To identify stabilizing and destabilizing structural elements for alkene-chelated ruthenium complexes, we explored the reaction of various 1,*n*-diynes with **G-II** in CH_2Cl_2 at 45 °C (Table 1). In the presence of 1-octene (3 equiv), treating **6a** with **G-II** generated the hexyl group-incorporated alkene-chelate **10b** in 96% yield. This implies that the reaction of **G-II** with 1-octene is faster than that with diyne **6a**. However, with vinyl ferrocene (3 equiv) under otherwise identical conditions, ferrocene-containing complex **10c** was obtained along with **10a** in a 3.5:1 ratio (84% yield).[23] X-ray crystallographic data of **10c** shows that replacing the phenyl group in **10a** with a ferrocenyl group does not perturb the original structure. With the Grubbs−Hoveyda second-generation complex (**HG-II**), the diyne **6a** formed the chelate **10d** in 88% yield (*E*:*Z* = 14:1) where the isopropoxy ether does not interact with the metal center. Treating 1,6-diynes containing a *gem*-dimethyl group with **G-II**, however, generated mostly oligomers from which the alkene-chelate **10e** was isolated only in 5% yield and none of **10f** was obtained. The enlarged bond angle between the carbenic carbon and the *gem*-dimethylated carbon of the fused five-membered ring (126°) compared to the

https://dx.doi.org/10.1021/acscatal.0c04972
ACS Catal. 2021, 11, 1977−1987

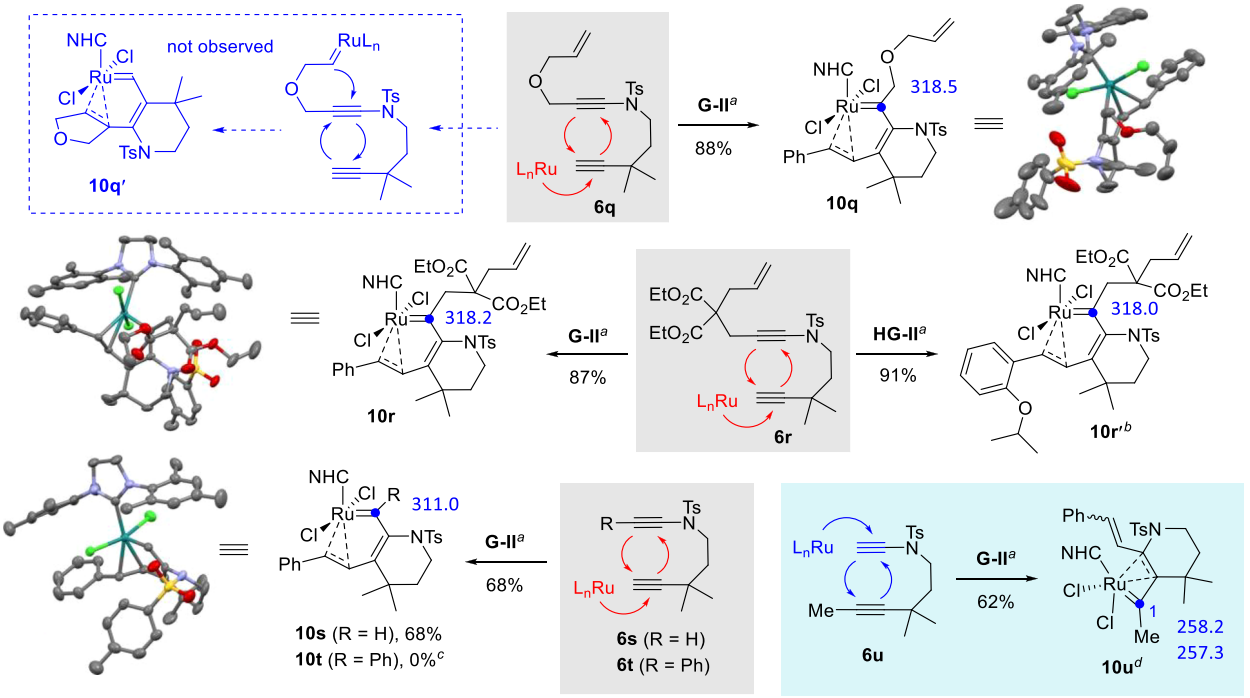

Figure 4. Unusual mode of RCM of ynamide-tethered 1,7-diynes to generate alkene-chelates. [a]**G-II** or **HG-II** (0.8 equiv), CH_2Cl_2, 45 °C (reported yields are isolated yields). [b]The structure was confirmed by X-ray crystallography. [c]Decomposition of the starting material. [d]A mixture of *E*:*Z* isomer (4:1) and each isomer displays the carbenic ^{13}C-signals at 258.2 and 257.3 ppm. The differently colored arrow represents the propagation of the ruthenium alkylidene along the π-bonds with the red-colored arrow representing the initiation from the more hindered alkyne and the blue arrow indicating initiation from the electron-rich ynamide.

corresponding six-membered ring-fused chelate (120°) may weaken the *exo*-Thorpe−Ingold effect. We surmised that replacement of the *gem*-dimethyl group in **10f** with a bulkier substituent such as an adamantyl moiety would reconstitute the proper steric effect.[24] Indeed, the adamantyl-substituted alkene-chelate **10g** was isolated in 54% yield, and the corresponding six-membered ring-fused alkene-chelate **10h** was obtained in much higher yield (78%). Replacing the *gem*-dimethyl carbon moiety with a diphenylsilyl group along with an additional *gem*-dimethyl group in the five-membered ring turned out to be more effective to promote alkene chelation to provide **10i** in 82% yield. From silyl ether-tethered 1,7- and 1,8-diynes, six- and seven-membered cyclic silyl ether-fused chelates **10j**−**10l** were generated efficiently.[25] The RCM initiated from an alkene tethered to 1,*n*-diynes followed by tandem enyne RCM provided ruthenium alkylidenes **10m**−**10o** that contain a chelated trisubstituted cyclic alkene. Unexpectedly, however, the all-carbon *gem*-dimethyl-containing intermediate **7p** did not undergo the seven-membered ring-forming RCM to generate **10p**; instead, it terminates with methylene transfer to provide **10p′** as the final product. This is in stark contrast to the formation of **10o** linked with a diphenylsilyl-tethered system, which clearly shows that the diphenylsilyl moiety plays a dual role as a *gem*-dialkyl surrogate to exert the *exo*-Thorpe−Ingold effect and as a promoter of RCM through the Thorpe−Ingold effect.[26]

Reaction Profile for Ynamide-Tethered 1,*n*-Diynes. To examine the electronic effect on the alkene to chelate with the ruthenium center, an ynamide tether is introduced to 1,*n*-diynes such that after RCM, an enamide moiety would be installed in the final ruthenium alkylidene product (Figure 4). According to a common reactivity, it is expected that the alkene-tethered 1,7-endiyne **6q** should initiate a tandem RCM from the alkene to generate the chelate **10q′**. In contrast, an initiation at the sterically most hindered neopentynyl site followed by RCM and chelation of the propagating ruthenium alkylidene with the styryl moiety provided **10q** in 88% yield. This unique mode of initiation at the alkyne of a neopentynyl nature is unprecedented, which may involve unusual chelation of ruthenium alkylidene between the two alkynes. Also, it is surprising that the tethered alkene remains intact without participating in RCM. Similarly, treatment of allylmalonyl-tethered diyne **6r** with **G-II** and **HG-II** generated alkene-chelates **10r** and **10r′** in 87 and 91% yields, respectively, while **G-I** failed to undergo an initiation. With the 1,7-diyne **6s** containing two terminal alkynes, the initiation occurred favorably at the more sterically hindered neopentynyl alkyne over the unhindered electron-rich terminal ynamide, generating the chelate **10s** (68%), while the structurally similar diyne **6t** containing a phenyl substituent only decomposed under the same conditions. On the other hand, the 1,7-diyne **6u** containing a terminal ynamide and a methyl substituent on the other alkyne underwent initiation at the terminal ynamide to provide the η^3-vinyl alkylidene complex **10u** in 62% yield (*E*:*Z* = 4:1). The complex **10u** displays the ^{13}C-signals at 258.2 and 257.3 ppm (*E*:*Z* mixture) for the carbenic carbon C1, which corresponds to the ^{13}C-signal range of η^3-vinyl chelated carbenes (230−285 ppm), whereas 1,5-chelates **10q**−**10s** display the carbenic ^{13}C-signals higher than 310 ppm. The formation of η^3-vinyl chelate from **6u** can be justified by an alternative initiation from the terminal ynamide to form the corresponding enamide moiety where the connectivity of the *N*-Ts is optimally disposed to provide an electronic driving force for the chelation similar to that in complexes **13** in Table 2.

Reaction Profile of 1,*n*-Enynes to Generate η^3-Vinyl Alkylidene Chelates. Although we expected that a relatively electron-rich enamide might chelate with the ruthenium center

https://dx.doi.org/10.1021/acscatal.0c04972
ACS Catal. 2021, 11, 1977−1987

Table 2. RCM of 1,*n*-Enynes to Form η^3-Vinyl Alkylidene Chelates

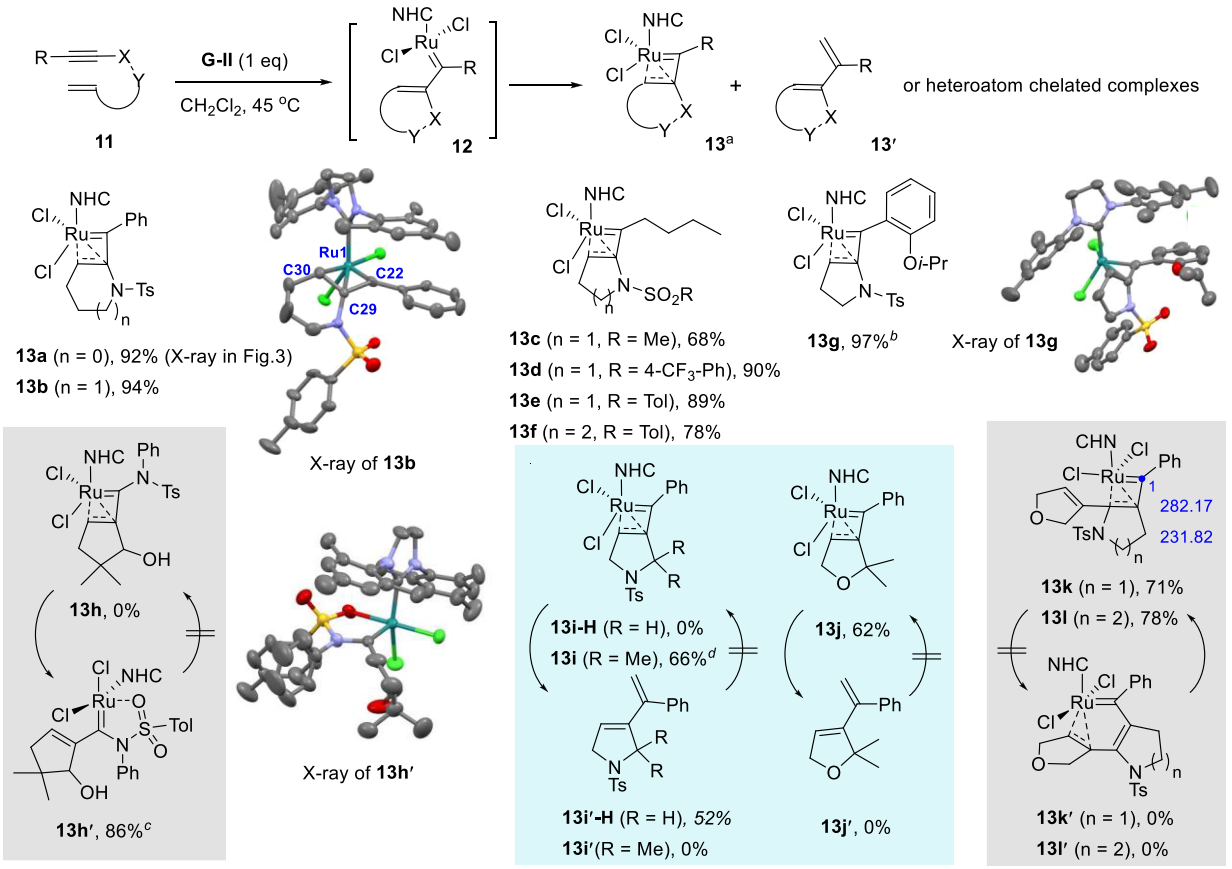

[a]Isolated yield. [b]The η^3-vinyl chelation was confirmed by X-ray crystallographic analysis. [c]Two chlorides are in a cis relationship. [d]82% yield based on the recovered starting material.

to form a η^3-vinyl alkylidene, complexes **10q**−**10s** in Figure 4 chelated with the distal alkene most likely due to the favorable geometry of forming 1,5-chelates over strained η^3-vinyl alkylidenes. We suspect that by removing this distal alkene, the ruthenium center would interact with the proximal enamide. With this hypothesis in mind, we explored the reaction of various 1,*n*-enynes containing an ynamide tether (Table 2).[27] Gratifyingly, treating 1,6- and 1,7-enyne containing a sulfonamide tether with **G-II** generated alkylidene chelates **13a** and **13b** in 92 and 94% yields, respectively. The X-ray crystallographic analysis of these complexes confirmed the η^3-vinyl chelation where the two chloride ligands are in a cis relationship. The true η^3-chelation mode of the complex **13b** can be confirmed from its X-ray structure, which shows delocalized bonding between C22, C29, and C30. The C29−C30 bond length is 1.395 Å, which is somewhat longer than typical C=C bonds (~1.35 Å), and the C22−C29 bond length is 1.44 Å, which is shorter than typical C−C bonds (~1.55 Å). X-ray structures of other complexes of this type also show true η^3-chelation mode (see the Supporting Information). Subtle electronic and structural changes including the tether size, nature of sulfonamide, and the substituent on the alkyne were tolerant and η^3-vinyl chelates **13c**−**13f** were obtained in high yields. To examine the possibility of competing chelation by an enamide and an ether functionality, a 2-isopropoxyphenyl-substituted enynamide was employed with a prediction of forming a five-membered ring chelate by the isopropoxy group. However, the obtained complex was the η^3-vinyl chelate **13g**, proved by X-ray crystal structure analysis, whereas the expected oxygen chelation was established by installing a terminal ynamide such that the sulfonamide oxygen-chelated structure **13h′** was indeed isolated rather than the alkene-chelate **13h**. When there is no electronic driving force, the *exo*-Thorpe−Ingold effect by a *gem*-dimethyl moiety can be resorted to promote chelation. For example, without a *gem*-dimethyl group on the propargylic site, the metathesis product **13i′-H** (52% yield) was generated devoid of the η^3-vinyl chelate **13i-H**, whereas the corresponding *gem*-dimethyl-containing system provided the η^3-vinyl chelate **13i** in 66% yield without the metathesis product **13i′**. The presence of a *gem*-dimethyl group in **13i** prevents further [2 + 2] cycloaddition as the incipient ruthenacyclobutane is destabilized by the unfavorable syn-pentane interaction by the *gem*-dimethyl group; thus, no metathesis product is formed in this case. The similar complex **13j** was formed from a propargylic ether-tethered enyne in 62% yield, devoid of any metathesis product. Finally, competition between η^3-vinyl chelation and 1,5-chelation showed a preference for η^3-vinyl chelates in **13k** and **13l** over 1,5-chelates **13k′** and **13l′**, and this assignment is supported by the ^{13}C NMR signals of the carbenic C1 carbon at 282.17 and 231.82 ppm, respectively.

η^3-Vinyl Alkylidene Chelates with Heterocycles. The favorable interaction of the ruthenium center to form η^3-vinyl chelates with an enamide generated through RCM of ynamide prompted us to explore the chelation behavior of other electron-rich heterocycles such as pyrrole, furan, thiophene, and indole.[28] Toward this goal, we employed enyne RCM of **11m**−**11v** that

https://dx.doi.org/10.1021/acscatal.0c04972
ACS Catal. 2021, 11, 1977−1987

Table 3. Heteroatom Substituent Effect on the Formation of η^3-Vinyl Alkylidene Complexes

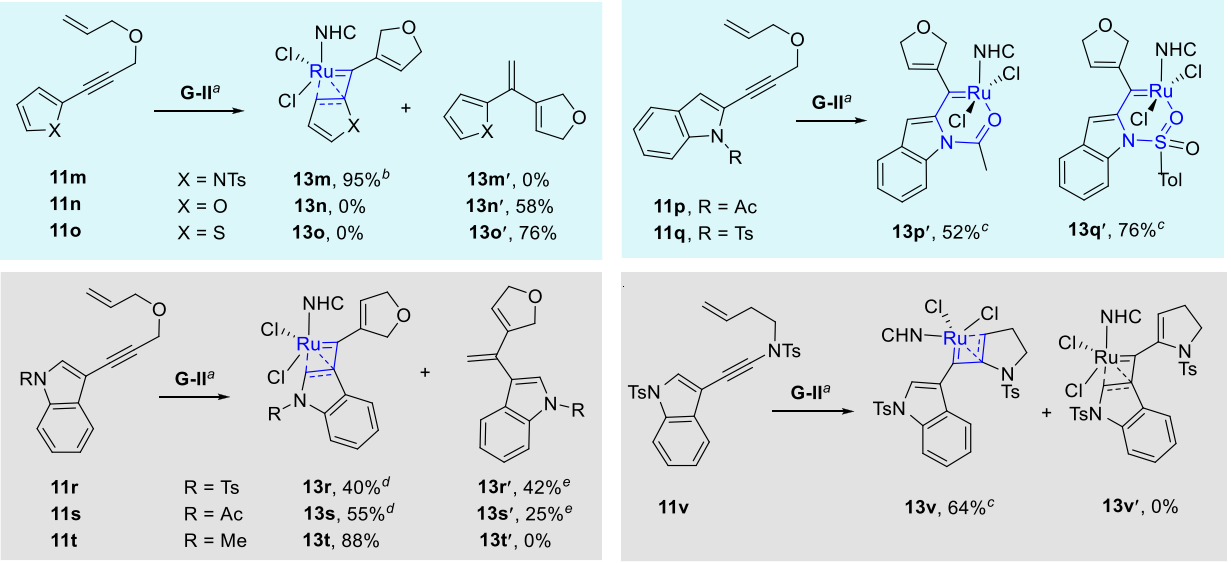

[a]**G-II** (0.8 equiv), CH_2Cl_2, 45 °C (reported yields are isolated yields). [b]Inseparable mixture of alkene- and sulfonamide-chelate in a 3:1 ratio. [c]Confirmed by X-ray crystallographic analysis. [d]The reaction was performed at 35 °C for 1 h. [e]NMR yields measured using internal standards.

contain preformed respective heteroaromatic systems (Table 3). Treating the 2-allyloxypropynyl pyrrole derivative **11m** gave the predominately alkene-chelated complex **13m** in 95% yield where a minor sulfonamide-chelate exists in a 3:1 ratio. On the other hand, the corresponding furan and thiophene derivatives **11n** and **11o** gave only metathesis products **13n′** and **13o′**. As opposed to the 2-pyrrole derivative **11m**, the corresponding 2-alkynyl indole derivatives **11p** and **11q** did not provide alkene-chelates, but only oxygen-chelates **13p′** and **13q′** were formed with an acetyl group and a sulfonyl group, respectively. This drastic change in chelation behavior can be attributed to the reduced electron density of the enamide moiety of an indole ring compared to pyrrole; therefore, the alkene chelation is superseded by oxygen chelation. By removing the possibility of oxygen chelation with geometrical constrains, only η^3-vinyl chelates **13r−13t** were obtained. The electron-withdrawing *p*-toluenesulfonyl and acetyl groups of **13r** and **13s** increase the lability of these complexes, which thus turn over to the metathesis products **13r′** and **13s′** in significant amounts compared to the methyl group-containing complex **13t**. The ynamide-tethered alkynyl indole **11v** was designed to examine the competition of ruthenium chelation between two similar enamide moieties of dihydropyrrole and indole. As expected, chelation occurred with the more electron-rich dihydropyrrole to form the η^3-vinyl complex **13v** without **13v′**, whose structure was unambiguously confirmed by X-ray crystallographic analysis.

Catalytic Activity: Structure/Activity Relationships. Having developed structurally diverse 1,5-alkene-chelates and η^3-vinyl chelates, we investigated the catalytic activities of these complexes for different metathesis processes.[29] First, we tested the catalytic activity of a variety of complexes for the RCM reaction of dimethyl diallylmalonate to establish a structure/activity relationship (see the Supporting Information, page s30). In general, the *trans*-1,5-alkene-chelated complexes fused with a five-membered ring such as **10g** and **10i** are active at ambient temperature (30 °C), but the corresponding six- or seven-membered ring-fused chelates **10h** and **10l** showed latent behaviors, which were inert at room temperature up to 45 °C but became active at higher temperature.[30] In comparison, η^3-vinyl chelates **13a−13f** are highly active at ambient temperature, whereas the η^3-vinyl chelate **2** was inactive for metathesis under otherwise identical conditions.[11] The catalytic activities of the latent 1,5-chelates were found to change drastically with variation in the tethering group (see the Supporting Information, pages s40−s44). For instance, in the RCM of dimethyl diallylmalonate catalyzed by these latent chelates at 80 °C in C_6D_6, the complex **10b** containing a *gem*-dimethyl group on the fused six-membered ring is less active (12% conversion) than the corresponding adamantyl-containing complex **10h** (57% conversion), yet the seven-membered ring-fused complex **10l** containing a diphenylsilyl group is much more reactive (99.1% conversion). The reactivity of the complexes is also significantly affected by the substituent on the carbenic carbon. Increasing the steric bulk of the substituent at the carbenic carbon decreases the reactivity significantly; thus, the η^3-vinyl chelate **13a** with a smaller butyl substituent[31] is much reactive than **13b** with a larger phenyl group (3 min vs 13 min for complete conversion at 45 °C). Sometimes, the presence of an alternate chelating group may shut the catalytic activity completely; for example, **10g** with an ortho-isopropoxyphenyl substituent is catalytically inactive, presumably due to a constant shuttling between the alkene-chelate and oxygen-chelate (see the Supporting Information, pages s31−s36).

Another important factor affecting the catalytic activity of η^3-vinyl chelates is the size of the fused ring; thus, the six-membered ring-fused complex **13b** (99% conversion in 3 min, 45 °C) is more reactive than the corresponding five-membered ring congener **13a** (96% conversion in 13 min, 45 °C). This reactivity difference can be justified by the structural difference in **13a** and **13b** revealed by their X-ray structures (Figure 5). While the five-membered ring of the bicyclo[3.1.0]hexane substructure in **13a** is unstrained, the six-membered ring of the bicyclo[4.1.0]-heptane moiety in **13b** is highly distorted to assume a boat conformation. Thus, the barrier for dissociation of the chelated alkene in **13b** should be lower than **13a**. The catalytic activity of

https://dx.doi.org/10.1021/acscatal.0c04972
ACS Catal. 2021, 11, 1977−1987

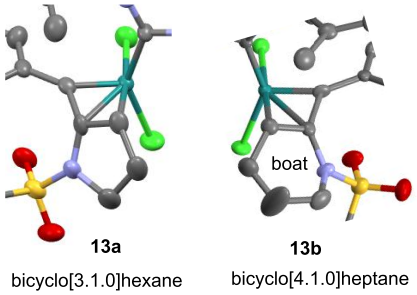

Figure 5. Partial structure of **13a** and **13b** from X-ray data.

oxygen-chelated complexes like **13p′** and **13q′** for RCM reactions was also tested; while the acetate chelate **13p′** did not show any activity, the corresponding sulfonamide chelate **13q′** was catalytically active at 45 °C (see the Supporting Information, pages s37−s39).

Benchmarking Catalytic Activity. After establishing a reactivity trend for the different types of alkene-chelates, we selected a subset of relatively more active complexes to benchmark their catalytic activity for various metathesis processes with respect to standard metathesis catalysts.

Accordingly, the reaction profile of these complexes was studied for the RCM of dimethyl diallylmalonate and dimethyl allylmethallylmalonate,[32] the CM of terminal alkene with acrylate,[33] and the ROMP of 1,5-cycloactadiene[34,35] (Figure 6a−d), and kinetic parameters including rate constants (k_{obs} and k_{rel}) and half-lives ($t_{1/2}$) were determined with reference to **G-II** (Figure 7). Among the catalysts tested for the RCM of dimethyl diallylmalonate, **10g** (k_{rel} = 9.64, 97.7% conversion) and **13f** (k_{rel} = 11.48, 98.6% conversion) showed the best performance. The

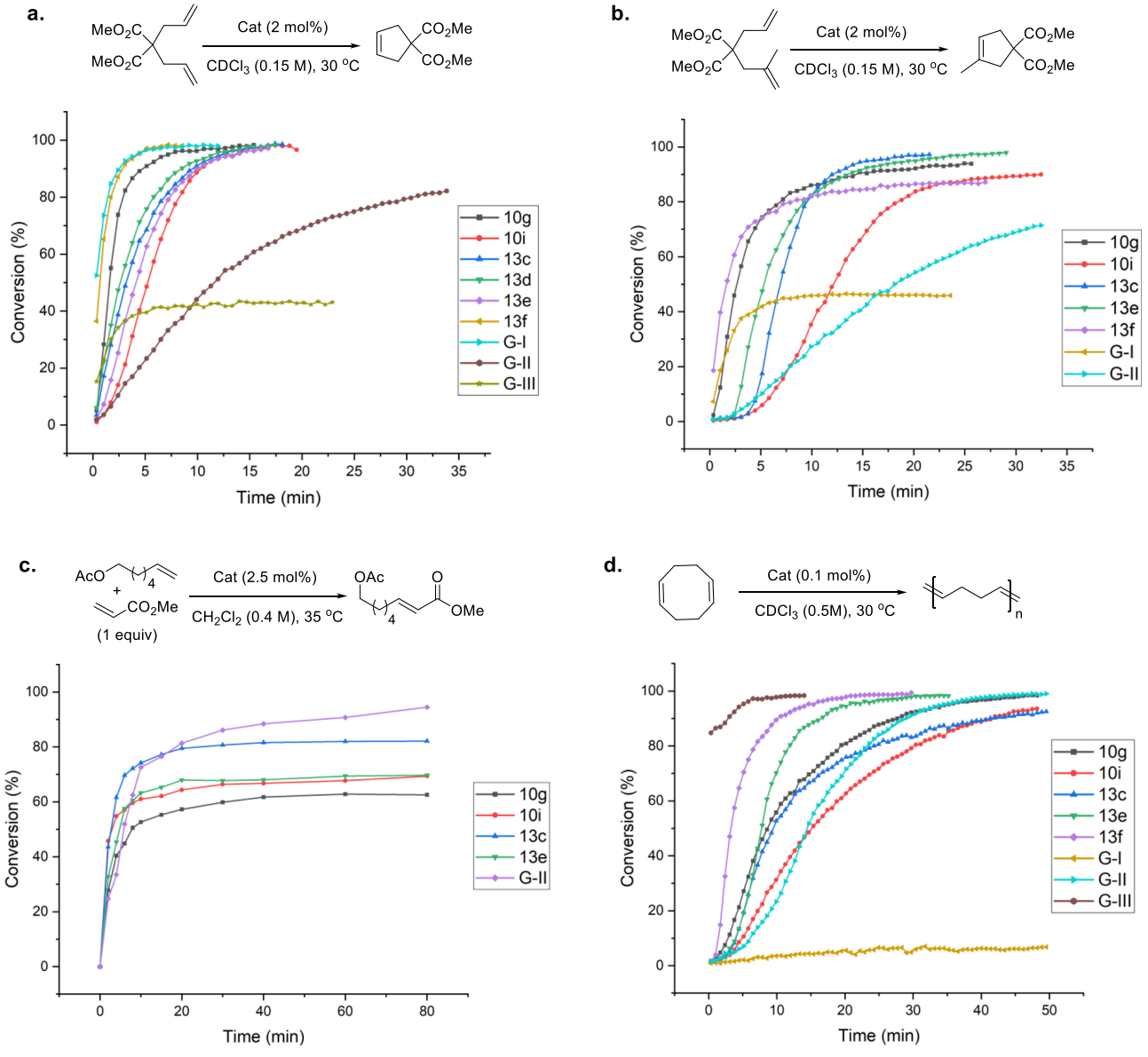

Figure 6. Catalytic activities of alkene-chelated ruthenium alkylidene complexes. The kinetic profile for each reaction was obtained by NMR spectroscopy (Bruker's pseudo 2D kinetics method) by equilibrating the NMR probe at requisite temperature. Each data point represents the average of three runs of individual experiment except for CM experiments where two runs were performed. (a) RCM profiles of dimethyl diallylmalonate at 30 °C in $CDCl_3$ (0.15 M). (b) RCM profiles of dimethyl allylmethallylmalonate at 30 °C in $CDCl_3$ (0.15 M). (c) CM profiles of 5-hexenyl acetate with methyl acrylate at 35 °C in CH_2Cl_2 (0.4 M). (d) ROMP profiles of 1.5-cyclooctadiene at 30 °C in $CDCl_3$ (0.5 M).

https://dx.doi.org/10.1021/acscatal.0c04972
ACS Catal. 2021, 11, 1977−1987

Latent Catalyst[a]	Active Catalyst							
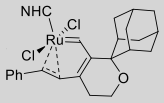				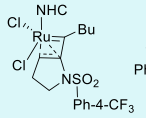	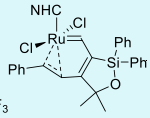	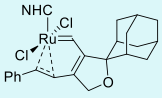		
10h	G-II	13c	13e	13d	10i	10g	13f	
k_{rel} ($CDCl_3$)[b] 0 (no initiation)	1.00	4.80	4.64	4.76	5.50	9.64	11.48	RCM (disubstituted olefin)
k_{rel} (CD_2Cl_2)[b, c]	1.00	3.74	3.48	3.83	3.63	3.57	5.98	
k_{rel} ($CDCl_3$)[b]	1.00	5.43	4.14		3.13	6.15	7.61	RCM (trisubstituted olefin)
k_{rel} ($CDCl_3$)[b]	1.00	0.42	1.35		0.75	0.52	1.66	ROMP

Figure 7. Reactivity order of selected alkene-chelates for different metathesis processes. [a]Latent catalysts involve the 1,5-chelates with six- or seven-membered rings. These complexes do not show catalytic activity at room temperature and is only active at higher temperature. [b]The k_{rel} value represents the rate constant for a particular complex with respect to **G-II** for different metathesis processes. [c]The k_{rel} value for RCM of dimethyl diallylmalonate was also determined in CD_2Cl_2 for comparison with previously reported data.[29]

kinetics for RCM of dimethyl diallylmalonate was also studied in CD_2Cl_2 to compare with previously reported conditions.[29] In CD_2Cl_2, there was a great rate enhancement for standard metathesis catalysts like **G-II** and **G-III**, while the alkene-chelates demonstrated superior activity in both CD_2Cl_2 and $CDCl_3$. More specifically, alkene-chelates **13c**, **13d**, **13e**, and **10i** showed an enhancement in rate, while **10g** and **13f** showed a decrease in rate in CD_2Cl_2 compared to $CDCl_3$. In the RCM of dimethyl allylmethallylmalonate, catalysts **13c** (k_{rel} = 5.43, 97.0% conversion) and **13e** (k_{rel} = 4.14, 97.7% conversion) achieved near full conversion, although their k_{rel} values are lower than those of **10g** (k_{rel} = 6.15, 93.5% conversion) and **13f** (k_{rel} = 7.61, 87% conversion). In the CM of 5-hexenyl acetate with methacrylate, complexes **10g**, **13c**, and **13e** initiated the reaction with a higher rate than **G-II**, but the reactions slowed down and resulted in 63−82% conversion, while the conversion with **G-II** was 94%. In the ROMP of 1,5-cyclooctadiene, **13e** (k_{rel} = 1.38, 98% conversion) and **13f** (k_{rel} = 1.66, 99% conversion) provided near full conversion with a slightly higher rate compared to **G-II**.

Overall, these two different classes of alkene-chelated ruthenium alkylidenes, 1,5-alkene chelates, and η^3-vinyl chelates, if they have right combinations of structural elements, can display decent metathesis activity in different types of metathesis reactions with consistency. This compares favorably with the behaviors of typical Grubbs-type metathesis catalysts; for example, **G-III** is an excellent catalyst for ROMP but shows relatively low reactivity toward RCM reactions (Figure 6a,d).[36]

CONCLUSIONS

We have developed a general approach to promote the formation of alkene-chelated ruthenium alkylidenes relying on ring-closing enyne metathesis of 1,*n*-diynes and 1,*n*-enynes. Because of the tandem nature of enyne metathesis to form these complexes, steric and electronic variation can be easily introduced to engineer the stability and catalytic activities of these new complexes. The crucial structural element that facilitates 1,5-alkene chelation is the *exo*-Thorpe−Ingold effect of a *gem*-dialkyl substituent. On the other hand, the driving force for the formation of geometrically constrained η^3-vinyl alkylidene is provided by an electronic activation on the chelating alkene. The stability and reactivity of these alkene-chelated complexes can be modulated not only by these crucial structural elements but also by other auxiliaries. For example, five-membered ring-fused 1,5-chelates are more reactive than the corresponding six- and seven-membered ring-fused congeners. In general, η^3-vinyl alkylidenes and 1,5-chelates fused with a five-membered ring display superior catalytic activity in RCM, CM, and ROMP reactions compared to other alkene-chelates. Another meritorious feature of these new alkene-chelated ruthenium alkylidenes is their consistency in performing different types of metathesis processes. The versatility of catalysts[37] for different types of reactions, which many standard metathesis catalysts lack, is an important goal in developing new catalysts. Thus, these alkene-chelated ruthenium alkylidene complexes might provide a sustainable platform to further develop catalysts of enhanced catalytic activity and versatility. This study not only demonstrated the possibility of generating novel alkene-chelates by exploiting nonproductive coordination events in enyne metathesis but also discovered new metathesis catalysts with high activity, which might find broad utility in organic synthesis and polymer chemistry.

ASSOCIATED CONTENT

Supporting Information

The Supporting Information is available free of charge at https://pubs.acs.org/doi/10.1021/acscatal.0c04972.

Experimental details for all reactions and characterization data for all products (PDF)

Crystallographic data deposited at the Cambridge Crystallographic Data Centre under deposition number 2018298 (**10a**) (CIF)

Crystallographic data deposited at the Cambridge Crystallographic Data Centre under deposition number 2021743 (**10c**) (CIF)

Crystallographic data deposited at the Cambridge Crystallographic Data Centre under deposition number 2018914 (**10d**) (CIF)

Crystallographic data deposited at the Cambridge Crystallographic Data Centre under deposition number 2018302 (**10l**) (CIF)

https://dx.doi.org/10.1021/acscatal.0c04972
ACS Catal. 2021, 11, 1977−1987

Crystallographic data deposited at the Cambridge Crystallographic Data Centre under deposition number 2018588 (**10q**) (CIF)

Crystallographic data deposited at the Cambridge Crystallographic Data Centre under deposition number 2018303 (**10r**) (CIF)

Crystallographic data deposited at the Cambridge Crystallographic Data Centre under deposition number 2018594 (**10r′**) (CIF)

Crystallographic data deposited at the Cambridge Crystallographic Data Centre under deposition number 2018596 (**10s**) (CIF)

Crystallographic data deposited at the Cambridge Crystallographic Data Centre under deposition number 2018283 (**13a**) (CIF)

Crystallographic data deposited at the Cambridge Crystallographic Data Centre under deposition number 2018831 (**13b**) (CIF)

Crystallographic data deposited at the Cambridge Crystallographic Data Centre under deposition number 2018917 (**13g**) (CIF)

Crystallographic data deposited at the Cambridge Crystallographic Data Centre under deposition number 2021918 (**13h′**) (CIF)

Crystallographic data deposited at the Cambridge Crystallographic Data Centre under deposition number 2019504 (**13p′**) (CIF)

Crystallographic data deposited at the Cambridge Crystallographic Data Centre under deposition number 2019503 (**13q′**) (CIF)

Crystallographic data deposited at the Cambridge Crystallographic Data Centre under deposition number 2019480 (**13v**) (CIF)

AUTHOR INFORMATION

Corresponding Author

Daesung Lee − *Department of Chemistry, University of Illinois at Chicago, Chicago, Illinois 60607, United States;* orcid.org/0000-0003-3958-5475; Email: dsunglee@uic.edu

Authors

Saswata Gupta − *Department of Chemistry, University of Illinois at Chicago, Chicago, Illinois 60607, United States*

Venkata R. Sabbasani − *Department of Chemistry, University of Illinois at Chicago, Chicago, Illinois 60607, United States;* orcid.org/0000-0002-4558-2812

Siyuan Su − *Department of Chemistry, University of Illinois at Chicago, Chicago, Illinois 60607, United States*

Donald J. Wink − *Department of Chemistry, University of Illinois at Chicago, Chicago, Illinois 60607, United States;* orcid.org/0000-0002-2475-2392

Complete contact information is available at: https://pubs.acs.org/10.1021/acscatal.0c04972

Author Contributions

‡S.G. and V.R.S. contributed equally to this work.

Notes

The authors declare no competing financial interest.

Copies of the data can be obtained free of charge via https://www.ccdc.cam.ac.uk/structures/.

ACKNOWLEDGMENTS

The Mass Spectrometry Laboratory at UIUC is acknowledged. Prof. Neal Mankad of UIC, Chemistry Department, is acknowledged for helping to analyze the X-ray structures of **13a** and **13b**.

REFERENCES

(1) (a) Fürstner, A. Olefin metathesis and beyond. *Angew. Chem., Int. Ed.* **2000**, *39*, 3012−3043. (b) Fürstner, A. Teaching metathesis "simple" stereochemistry. *Science* **2013**, *341*, 1229713−1221364. (c) Hoveyda, A. H.; Zhugralin, A. R. The remarkable metal-catalysed olefin metathesis reaction. *Nature* **2007**, *450*, 243−251.

(2) (a) Mol, J. C. Industrial applications of olefin metathesis. *J. Mol. Catal. A: Chem.* **2004**, *213*, 39−45. (b) Grubbs, R. H. Olefin metathesis catalysts for the preparation of molecules and materials (Nobel lecture). *Angew. Chem., Int. Ed.* **2006**, *45*, 3760−3765. (c) Clavier, H.; Grela, K.; Kirschning, A.; Mauduit, M.; Nolan, S. P. Sustainable concepts in olefin metathesis. *Angew. Chem., Int. Ed.* **2007**, *46*, 6786−6801. (d) Higman, C. S.; Lummiss, J. A. M.; Fogg, D. E. Olefin metathesis at the dawn of implementation in pharmaceutical and specialty-chemicals manufacturing. *Angew. Chem., Int. Ed.* **2016**, *55*, 3552−3565.

(3) (a) Vougioukalakis, G. C.; Grubbs, R. H. Ruthenium-based heterocyclic carbene-coordinated olefin metathesis catalysts. *Chem. Rev.* **2010**, *110*, 1746−1787. (b) Ogba, O. M.; Warner, N. C.; O'Leary, D. J.; Grubbs, R. H. Recent advances in ruthenium−based olefin metathesis. *Chem. Soc. Rev.* **2018**, *47*, 4510−4544.

(4) (a) Mori, M. Synthesis of natural products and related compounds using enyne metathesis. *Adv. Synth. Catal.* **2007**, *349*, 121−135. (b) Grubbs, R. H. *Metathesis in natural product synthesis: strategies, substrates and catalysts*; John Wiley & Sons: 2011. (c) Prunet, J. Progress in metathesis through natural product synthesis. *Eur. J. Org. Chem.* **2011**, *2011*, 3634−3647. (d) Werrel, S.; Walker, J. C. L.; Donohoe, T. J. Application of catalytic Z-selective olefin metathesis in natural product synthesis. *Tetrahedron Lett.* **2015**, *56*, 5261−5268.

(5) (a) Fürstner, A.; Thiel, O. R.; Lehmann, C. W. Study concerning the effects of chelation on the structure and catalytic activity of ruthenium carbene complexes. *Organometallics* **2002**, *21*, 331−335. (b) Wakamatsu, H.; Blechert, S. A Highly Active and Air-Stable Ruthenium Complex for Olefin Metathesis. *Angew. Chem., Int. Ed.* **2002**, *41*, 794−796. (c) Fürstner, A.; Davies, P. W.; Lehmann, C. W. Bidentate ruthenium vinylcarbene catalysts derived from enyne metathesis. *Organometallics* **2005**, *24*, 4065−4071.

(6) (a) Tzur, E.; Szadkowska, A.; Ben-Asuly, A.; Makal, A.; Goldberg, I.; Woźniak, K.; Grela, K.; Lemcoff, N. G. Studies on Electronic Effects in O-, N- and S- Chelated Ruthenium Olefin-Metathesis Catalysts. *Chem. − Eur. J.* **2010**, *16*, 8726−8737. (b) Vidavsky, Y.; Anaby, A.; Lemcoff, N. G. Chelating alkylidene ligands as pacifiers for ruthenium catalysed olefin metathesis. *Dalton Trans.* **2012**, *41*, 32−43. (c) Duan, Y.; Wang, T.; Xie, Q.; Yu, X.; Guo, W.; Wang, J.; Liu, G. Highly efficient nitrogen chelated ruthenium carbene metathesis catalysts. *Dalton Trans.* **2016**, *45*, 19441−19448. (c) Ivry, E.; Nechmad, N. B.; Baranov, M.; Goldberg, I.; Lemcoff, N. G. Influence of Anionic Ligand Exchange in Latent Sulfur-Chelated Ruthenium Precatalysts. *Inorg. Chem.* **2018**, *57*, 15592−15599. (d) Nechmad, N. B.; Lemcoff, N. G. Sulfur-Chelated Ruthenium Olefin Metathesis Catalysts. *Synlett* **2020**, DOI: 10.1055/s-0040-1707231.

(7) (a) Barbasiewicz, M.; Szadkowska, A.; Bujok, R.; Grela, K. Structure and activity peculiarities of ruthenium quinoline and quinoxaline complexes: Novel metathesis catalysts. *Organometallics* **2006**, *25*, 3599−3604. (b) Szadkowska, A.; Żukowska, K.; Pazio, A. E.; Woźniak, K.; Kadyrov, R.; Grela, K. Ruthenium Olefin Metathesis Catalysts Containing Six-Membered Sulfone and Sulfonamide Chelating Rings. *Organometallics* **2011**, *30*, 1130−1138. (c) Peeck, L. H.; Savka, R. D.; Plenio, H. Fast olefin metathesis at low catalyst loading. *Chem. − Eur. J.* **2012**, *18*, 12845−12853. (d) Barbasiewicz, M.; Michalak, M.; Grela, K. A New Family of Halogen-Chelated Hoveyda−Grubbs-Type Metathesis Catalysts. *Chem. − Eur. J.* **2012**, *18*, 14237−14241.

(8) (a) Keitz, B. K.; Endo, K.; Patel, P. R.; Herbert, M. B.; Grubbs, R. H. Improved ruthenium catalysts for Z-selective olefin metathesis. *J. Am. Chem. Soc.* **2012**, *134*, 693−699. (b) Khan, R. K. M.; Torker, S.; Hoveyda, A. H. Readily accessible and easily modifiable Ru-based catalysts for efficient and Z-selective ring-opening metathesis polymerization and ring-opening/cross-metathesis. *J. Am. Chem. Soc.* **2013**, *135*, 10258−10261. (c) Sabbasani, V. R.; Yun, S. Y.; Lee, D. Structure and reactivity of sulfonamide- and acetate-chelated ruthenium alkylidene complexes. *Org. Chem. Front.* **2016**, *3*, 939−943.

(9) (a) Garber, S. B.; Kingsbury, J. S.; Gray, B. L.; Hoveyda, A. H. Efficient and recyclable monomeric and dendritic Ru-based metathesis catalysts. *J. Am. Chem. Soc.* **2000**, *122*, 8168−8179. (b) Gessler, S.; Randl, S.; Blechert, S. Synthesis and metathesis reactions of a phosphine-free dihydroimidazole carbene ruthenium complex. *Tetrahedron Lett.* **2000**, *41*, 9973−9976.

(10) Tallarico, J. A.; Bonitatebus, P. J.; Snapper, M. L. Ring-opening metathesis A ruthenium catalyst caught in the act. *J. Am. Chem. Soc.* **1997**, *119*, 7157−7158.

(11) Trnka, T. M.; Day, M. W.; Grubbs, R. H. Novel η^3-vinylcarbene complexes derived from ruthenium-based olefin metathesis catalysts. *Organometallics* **2001**, *20*, 3845−3847.

(12) Anderson, D. R.; Hickstein, D. D.; O'Leary, D. J.; Grubbs, R. H. Model compounds of ruthenium−alkene intermediates in olefin metathesis reactions. *J. Am. Chem. Soc.* **2006**, *128*, 8386−8387.

(13) Song, J. A.; Park, B.; Kim, S.; Kang, C.; Lee, D.; Baik, M. H.; Grubbs, R. H.; Choi, T. L. Living polymerization caught in the act: direct observation of an arrested intermediate in metathesis polymerization. *J. Am. Chem. Soc.* **2019**, *141*, 10039−10047.

(14) Wang, K. P.; Yun, S. Y.; Lee, D.; Wink, D. J. Structure and reactivity of alkyne-chelated ruthenium alkylidene complexes. *J. Am. Chem. Soc.* **2009**, *131*, 15114−15115.

(15) (a) Benitez, D.; Tkatchouk, E.; Goddard, W. A., III Relevance of cis-and trans-dichloride Ru intermediates in Grubbs-II olefin metathesis catalysis ($H_2IMesCl_2Ru$=CHR). *Chem. Commun.* **2008**, *46*, 6194−6196. (b) Diesendruck, C. E.; Tzur, E.; Ben-Asuly, A.; Goldberg, I.; Straub, B. F.; Lemcoff, N. G. Predicting the Cis−Trans Dichloro Configuration of Group 15−16 Chelated Ruthenium Olefin Metathesis Complexes: A DFT and Experimental Study. *Inorg. Chem.* **2009**, *48*, 10819−10825. (c) Pump, E.; Poater, A.; Zirngast, M.; Torvisco, A.; Fischer, R.; Cavallo, L.; Slugovc, C. Impact of electronic modification of the chelating benzylidene ligand in cis-dichloro-configured second-generation olefin metathesis catalysts on their activity. *Organometallics* **2012**, *33*, 2806−2813. (d) Pump, E.; Cavallo, L.; Slugovc, C. A theoretical view on the thermodynamic cis−trans equilibrium of dihalo ruthenium olefin metathesis (pre-) catalysts. *Monatsh. Chem.* **2015**, *146*, 1131−1141.

(16) (a) Diver, S. T.; Giessert, A. J. Enyne metathesis (enyne bond reorganization). *Chem. Rev.* **2004**, *104*, 1317−1382. (b) Diver, S. T. Ruthenium vinyl carbene intermediates in enyne metathesis. *Coord. Chem. Rev.* **2007**, *251*, 671−701.

(17) Hansen, E. C.; Lee, D. Search for solutions to the reactivity and selectivity problems in enyne metathesis. *Acc. Chem. Res.* **2006**, *39*, 509−519.

(18) Anderson, D. R.; O'Leary, D. J.; Grubbs, R. H. Ruthenium−olefin complexes: effect of ligand variation upon geometry. *Chem. − Eur. J.* **2008**, *14*, 7536−7544.

(19) Stewart, I. C.; Benitez, D.; O'Leary, D. J.; Tkatchouk, E.; Day, M. W.; Goddard, W. A., III; Grubbs, R. H. Conformations of N-heterocyclic carbene ligands in ruthenium complexes relevant to olefin metathesis. *J. Am. Chem. Soc.* **2009**, *131*, 1931−1938.

(20) Jung, M. E.; Piizzi, G. *gem*-Disubstituent effect: Theoretical basis and synthetic applications. *Chem. Rev.* **2005**, *105*, 1735−1766.

(21) (a) Forbes, M. D. E.; Patton, J. T.; Myers, T. L.; Maynard, H. D.; Smith, D. W., Jr.; Schulz, G. R.; Wagener, K. B. Solvent-free cyclization of linear dienes using olefin metathesis and the Thorpe-Ingold effect. *J. Am. Chem. Soc.* **1992**, *114*, 10978−10980. (b) Kirkland, T. A.; Grubbs, R. H. Effects of olefin substitution on the ring-closing metathesis of dienes. *J. Org. Chem.* **1997**, *62*, 7310−7318. (c) Urbina-Blanco, C. A.; Skibiński, M.; O'Hagan, D.; Nolan, S. P. Accelerating influence of the *gem*-difluoromethylene group in a ring-closing olefin metathesis reaction. A Thorpe−Ingold effect? *Chem. Commun.* **2013**, *49*, 7201−7203. (d) Sabbasani, V. R.; Gupta, S.; Yun, S. Y.; Lee, D. A general approach for the formation of oxygen-chelated ruthenium alkylidene complexes relying on the Thorpe−Ingold effect. *Org. Chem. Front.* **2018**, *5*, 1532−1536.

(22) Mori, M.; Wakamatsu, H.; Saito, N.; Sato, Y.; Narita, R.; Sato, Y.; Fujita, R. Synthesis of cyclic dienamide using ruthenium-catalyzed ring-closing metathesis of ene−ynamide. *Tetrahedron* **2006**, *62*, 3872−3881.

(23) Maishal, T. K.; Sarkar, A. An air-stable, reusable, bimetallic version of Grubbs' catalyst for alkene metathesis. *Synlett* **2002**, *2002*, 1925−1927.

(24) Salvio, R.; Mandolini, L.; Savelli, C. Guanidine−guanidinium cooperation in bifunctional artificial phosphodiesterases based on diphenylmethane spacers; *gem*-dialkyl effect on catalytic efficiency. *J. Org. Chem.* **2013**, *78*, 7259−7263.

(25) (a) Miller, R. L.; Maifeld, S. V.; Lee, D. Ruthenium-catalyzed silyl ether formation and enyne metathesis sequence: Synthesis of siloxacycles from terminal alkenyl alcohols and alkynylsilanes. *Org. Lett.* **2004**, *6*, 2773−2776. (b) Park, S.; Kim, M.; Lee, D. Tandem sequence of cross metathesis−ring-closing metathesis reaction of alkynyl silyloxy-tethered enynes. *J. Am. Chem. Soc.* **2005**, *127*, 9410−9415. For reviews on silicon tethers: (c) Bols, M.; Skrydstrup, T. Silicon-tethered reactions. *Chem. Rev.* **1995**, *95*, 1253−1277. (d) Gauthier, D. R., Jr.; Zandi, K. S.; Shea, K. J. Disposable tethers in synthetic organic chemistry. *Tetrahedron* **1998**, *54*, 2289−2338.

(26) (a) Kim, Y. J.; Grimm, J. B.; Lee, D. Absence of the Thorpe−Ingold effect by *gem*-diphenyl groups in ring-closing enyne metathesis. *Tetrahedron Lett.* **2007**, *48*, 7961−7964. (b) Luh, T. Y.; Hu, Z. Thorpe−Ingold effect in organosilicon chemistry. *Dalton Trans.* **2010**, *39*, 9185−9192. (c) Čusak, A. Temporary Silicon-Tethered Ring-Closing Metathesis: Recent Advances in Methodology Development and Natural Product Synthesis. *Chem. − Eur. J.* **2012**, *18*, 5800−5824.

(27) Mori and co-workers have demonstrated the enyne metathesis of ynamides in the presence of ethylene at higher temperature. This might be due to arresting of the propagating species through chelation with the enamide moiety in the absence of ethylene at low temperature. (a) Saito, N.; Sato, Y.; Mori, M. Synthesis of cyclic dienamide using ruthenium-catalyzed ring-closing metathesis of ene-ynamide. *Org. Lett.* **2002**, *4*, 803−805. (b) Evano, G.; Coste, A.; Jouvin, K. Ynamides: versatile tools in organic synthesis. *Angew. Chem., Int. Ed.* **2010**, *49*, 2840−2859.

(28) Sadimenko, A. P. Organometallic compounds of pyrrole, indole, carbazole, phospholes, siloles, and boroles. *Adv. Heterocycl. Chem.* **2001**, *79*, 115−197.

(29) Ritter, T.; Hejl, A.; Wenzel, A. G.; Funk, T. W.; Grubbs, R. H. A standard system of characterization for olefin metathesis catalysts. *Organometallics* **2006**, *25*, 5740−5745.

(30) (a) Hejl, A.; Day, M. W.; Grubbs, R. H. Latent olefin metathesis catalysts featuring chelating alkylidenes. *Organometallics* **2006**, *25*, 6149−6154. (b) Kost, T.; Sigalov, M.; Goldberg, I.; Ben-Asuly, A.; Lemcoff, N. G. Latent sulfur chelated ruthenium catalysts: Steric acceleration effects on olefin metathesis. *J. Organomet. Chem.* **2008**, *693*, 2200−2203. (c) Ben-Asuly, A.; Tzur, E.; Diesendruck, C. E.; Sigalov, M.; Goldberg, I.; Lemcoff, N. G. A thermally switchable latent ruthenium olefin metathesis catalyst. *Organometallics* **2008**, *27*, 811−813. (d) Monsaert, S.; Vila, A. L.; Drozdzak, R.; Van Der Voort, P.; Verpoort, F. Latent olefin metathesis catalysts. *Chem. Soc. Rev.* **2009**, *38*, 3360−3372. (e) Ginzburg, Y.; Anaby, A.; Vidavsky, Y.; Diesendruck, C. E.; Ben-Asuly, A.; Goldberg, I.; Lemcoff, N. G. Widening the latency gap in chelated ruthenium olefin metathesis catalysts. *Organometallics* **2011**, *30*, 3430−3437.

(31) Lehman, S. E.; Wagener, K. B. Synthesis of ruthenium olefin metathesis catalysts with linear alkyl carbene complexes. *Organometallics* **2005**, *24*, 1477−1482.

(32) (a) Grubbs, R. H.; Miller, S. J.; Fu, G. C. Ring-closing metathesis and related processes in organic synthesis. *Acc. Chem. Res.* **1995**, *28*, 446−452. (b) Deiters, A.; Martin, S. F. Synthesis of oxygen- and

https://dx.doi.org/10.1021/acscatal.0c04972
ACS Catal. 2021, 11, 1977−1987

nitrogen-containing heterocycles by ring-closing metathesis. *Chem. Rev.* **2004**, *104*, 2199−2238.
(33) (a) Chatterjee, A. K.; Morgan, J. P.; Scholl, M.; Grubbs, R. H. Synthesis of functionalized olefins by cross and ring-closing metatheses. *J. Am. Chem. Soc.* **2000**, *122*, 3783−3784. (b) Chatterjee, A. K.; Choi, T. L.; Sanders, D. P.; Grubbs, R. H. A general model for selectivity in olefin cross metathesis. *J. Am. Chem. Soc.* **2003**, *125*, 11360−11370.
(34) (a) Bielawski, C. W.; Grubbs, R. H. Highly efficient ring-opening metathesis polymerization (ROMP) using new ruthenium catalysts containing N-heterocyclic carbene ligands. *Angew. Chem., Int. Ed.* **2000**, *39*, 2903−2906. (b) Slugovc, C. The ring opening metathesis polymerisation toolbox. *Macromol. Rapid Commun.* **2004**, *25*, 1283−1297. (c) Bielawski, C. W.; Grubbs, R. H. Living ring-opening metathesis polymerization. *Prog. Polym. Sci.* **2007**, *32*, 1−29.
(35) Song, K.; Kim, K.; Hong, D.; Kim, J.; Heo, C. E.; Kim, H. I.; Hong, S. H. Highly active ruthenium metathesis catalysts enabling ring-opening metathesis polymerization of cyclopentadiene at low temperatures. *Nat. Commun.* **2019**, *10*, 3860−3869.
(36) (a) Camm, K. D.; Martinez Castro, N.; Liu, Y.; Czechura, P.; Snelgrove, J. L.; Fogg, D. E. Tandem ROMP−hydrogenation with a third-generation Grubbs catalyst. *J. Am. Chem. Soc.* **2007**, *129*, 4168−4169. (b) Kang, E. H.; Yu, S. Y.; Lee, I. S.; Park, S. E.; Choi, T. L. Strategies to enhance cyclopolymerization using third-generation Grubbs catalyst. *J. Am. Chem. Soc.* **2014**, *136*, 10508−10514. (c) Yasir, M.; Liu, P.; Tennie, I. K.; Kilbinger, A. F. M. Catalytic living ring-opening metathesis polymerization with Grubbs' second- and third-generation catalysts. *Nat. Chem.* **2019**, *11*, 488−494.
(37) (a) Vehlow, K.; Maechling, S.; Köhler, K.; Blechert, S. Versatile Ru-based metathesis catalysts designed for both homogeneous and heterogeneous processes. *J. Organomet. Chem.* **2006**, *691*, 5267−5277. (b) Dumas, A.; Tarrieu, R.; Vives, T.; Roisnel, T.; Dorcet, V.; Baslé, O.; Mauduit, M. A versatile and highly Z-Selective olefin metathesis ruthenium catalyst based on a readily accessible *N*-heterocyclic carbene. *ACS Catal.* **2018**, *8*, 3257−3262.

https://dx.doi.org/10.1021/acscatal.0c04972
ACS Catal. 2021, 11, 1977−1987